The influence of oxygen on the color of zirconium oxynitrides thin films

P. Carvalho, F. Vaz, L. Rebouta

University of Minho, Physics Dept., Azurém, 4800-058 Guimarães, Portugal

Outline

- Motivation
- Film preparation
  - Deposition system.
  - Deposition parameters
- Characterization techniques

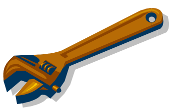

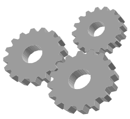

- Results.

  - Composition
  - Structure
  - Deposition rate
  - Electrical resistivity
  - Color
  - Residual stress
  - Hardness
  - Bond characteristics
- Conclusions.

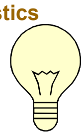

1. Motivation

- Develop a simple and easy way to prepare decorative thin film system

• 1 target

• 1 gas mixture

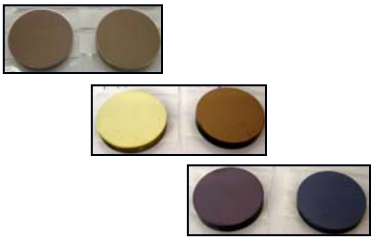

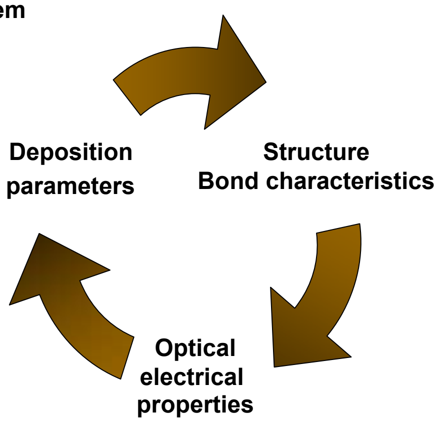

2. Film preparation

Base pressure.	1-3x10^{-4} Pa
Working pressure.	3-4x10^{-1} Pa
Target/substrate dist.	7 cm
Bias voltage	-75 to 0 V
Target current density	1x10^{-2} A/cm^2
Gas mixture	4 → 17.5 sccm

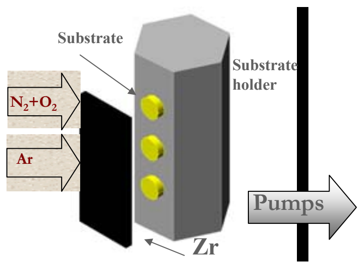

3. Characterization techniques

- **Basic**
  - Composition - RBS
  - Thickness - BC
- **Structure**
  - θ/2θ XRD
  - GIXRD - θ = 2º

  Phase formation
  Crystallinity
  Preferential orientation

- **Electrical**
  - Resistivity - four point probe method
- **Color and reflectivity**
  - CIELAB 1976 colour space
- **Bond characteristics**
  - FTIR
- **Mechanical**
  - Berkovich nanoindenter – Hardness
  - Deflection - Stress

4. Results

4.1 Composition and deposition rate - Mixture 2

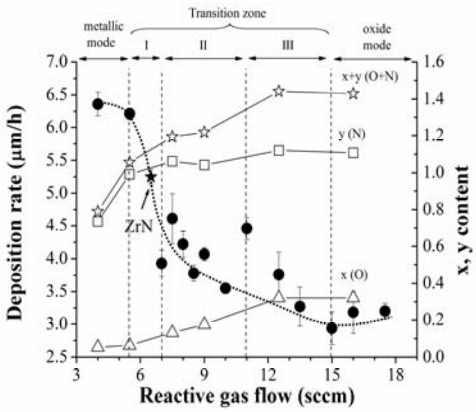

ion bombardment reduces the oxygen fraction in the samples "preferential re-sputtering"

3 different zones

- ❖ **metallic mode zone**
  - ⬆ Deposition rate
  - (N+O)/Zr ≤ 1
- ❖ **transition zone**
  - ⬇ Deposition rate
    Target poisoning
  - ⬆ concentration of non-metallic elements
- ❖ **oxynitride mode zone**
  - high concentration of non-metallic elements
  - Low deposition rate

4. Results

4.1 Color

zone 1 (5→10 sccm)

a* const
b* ⬆

zone 2 (10→13 sccm)

a* ⬇
b* ⬆→⬇

zone 3 (13→15 sccm)

a* ≈ const
b* ≈ const
Tendency to Inter. color

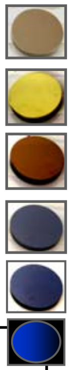

Mixture 1

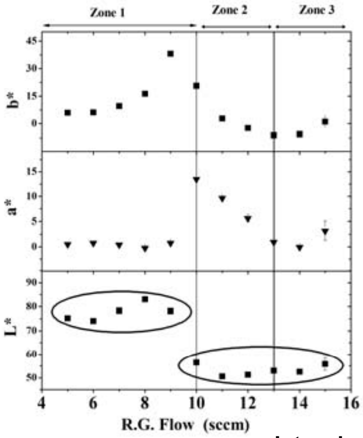

3 distinct behaviours of colorimetric coordinates a* and b*

2 distinct regions of Lightness (L*)

⬇ L*

≠ interaction of material with incident light

4. Results

Mixture 2

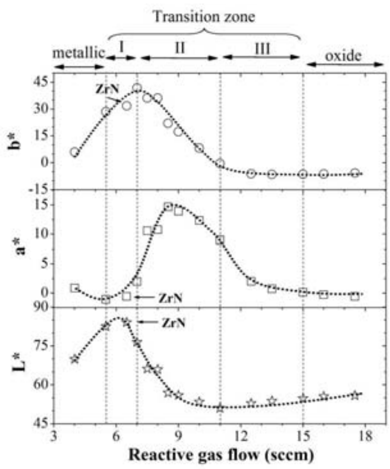

metallic mode zone
Light-yellow

transition zone I
Golden

transition zone II
Red-brownish

transition zone III and oxynitride zone
Dark blue

4. Results

Mixture 2
Color: *influence of oxygen fraction*

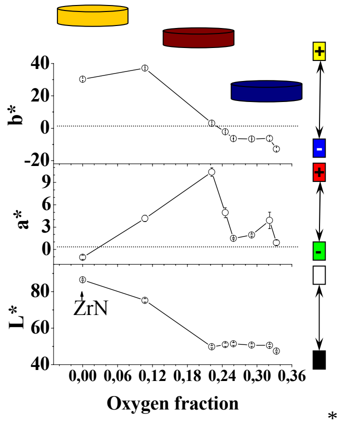

Results revealed:

- Coatings vary from **bright yellow-pink**, to **red-brownish** at intermediate oxygen fractions and **dark blue** for the highest oxygen fractions.

  A significant decrease in the brightness or brilliance, L*, with increasing oxygen fraction

strong dependence of colour on the oxygen fraction

Introduction of oxygen in ZrN

* f_{O2} = CO/(CO+CN)

4. Results

Mixture 2
Color: influence of bias voltage *(! and oxygen fraction)*

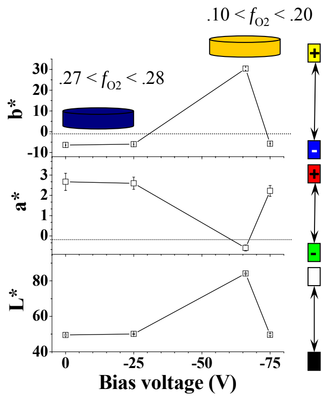

Results revealed:

- Sample prepared at – 66V (f_{O2} ~ 0.20) has an oxygen fraction ~ to $ZrN_{.91}O_{.26}$ (f_{O2} ~ 0.22) prepared at – 50 V

but very different colour parameters:

L* ~ 80 in comparison to ~ 50 for $ZrN_{.91}O_{.26}$
a* ~ -0.5 in comparison to ~ 10 for $ZrN_{.91}O_{.26}$
b* ~ 30 in comparison to ~ 5 for $ZrN_{.91}O_{.26}$

- **strong dependence of colour on the oxygen fraction**
- **Ion bombardment conditions**
- **stresses**

Type of bonds…

* f_{O2} = CO/(CO+CN)

4. Results

4.2 Structure

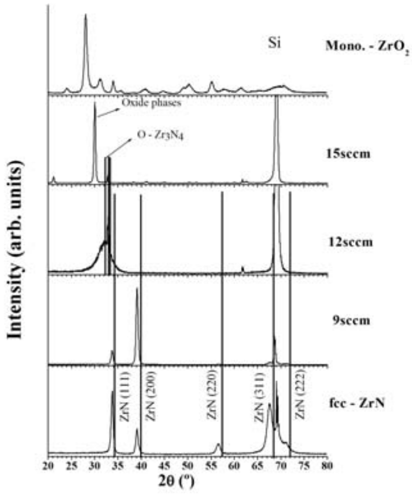

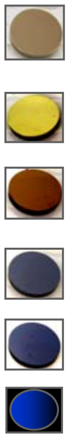

zone 1 (5→10 sccm)

high values of L*

↓ Intraband electronic transitions

ZrN with a rock salt structure

zone 2 (10→13 sccm)

low values of L*

↓ Interband electronic transitions

Poorly crystallized $O\text{-}Zr_3N_4$ - type structure

zone 3 (13→15 sccm)

zirconium oxynitride

•Cubic- ZrO_xN_y

4. Results

4.3 Reflectivity

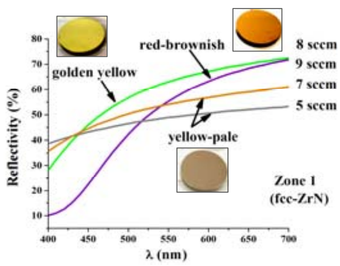

Predominant intraband electronic transitions

- ⇧ overall reflectivity until 8 sccm
- decrease of the nitrogen vacancy, in the ZrN lattice
- ⇧ Reactive gas flow 8 sccm (stoichiometric ZrN golden color)
- ⇩ overall reflectivity R.G. flow higher than 8 sccm
- ⇩ free *d* electrons from zirconium
- ⇩ efficiency of re-emission of the radiation by the electrons

With the changes in the structure from fcc-ZrN to $O\text{-}Zr_3N_4$

Significant ⇩ overall reflectivity

change in the interaction of material with incident light

from intra- to interband electronic transitions

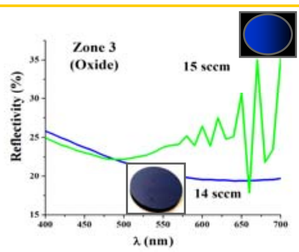

4. Results

4.4 Electrical - resistivity

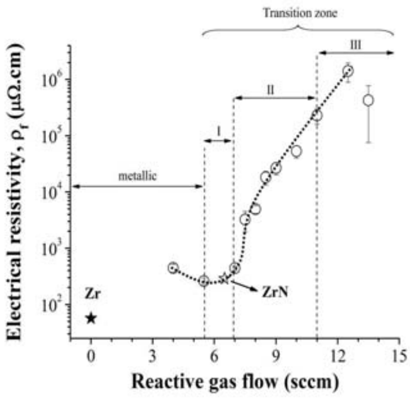

metallic zone **transition zone I**

low values of resistivity

↓

metallic nature of the films

transition zone I ⟶

⬆ resistivity

↓

⬇ the metallic bond contribution

⬆ covalent Zr-N and ionic Zr-O bonds

4. Results

4.5 Resistivity as a function of temperature

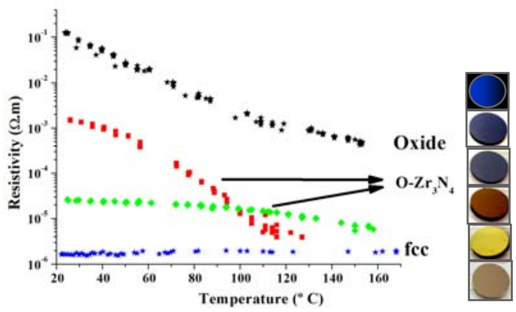

Zone 1 - Rock salt structure

low values of resistivity

metallic nature of the films

Zone 2 - $O\text{-}Zr_3N_4$ structure

⬆ resistivity

Change on the evolution of the resistivity with the temperature

Conductor ➡ semicondutor/insulating electrical behavior

⬇ the metallic bond contribution

⬆ covalent Zr-N and ionic Zr-O bonds

Zone 3 - Oxynitride

⬆ resistivity

formation of oxynitride insulating phases

4. Results

4.6 Bond characteristics

FTIR

Oxynitride

Monoclinic- ZrO_2 ???

O-Zr_3N_4

Rock salt structure

high conductivity

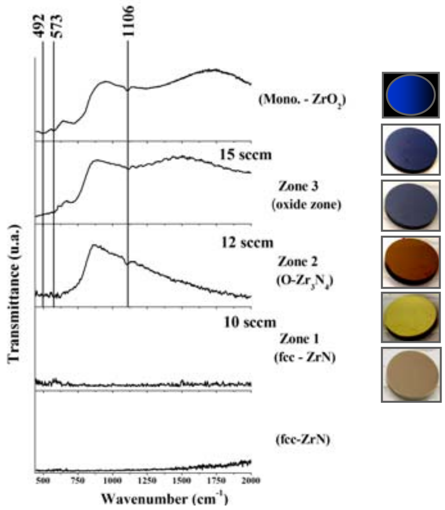

4. Results

4.7 Mechanical - stress

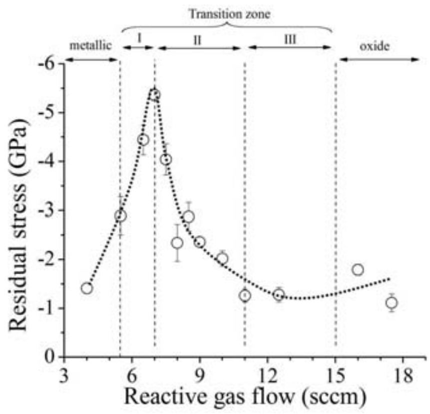

Low reactive gas flow

⬆ **residual stress**

⬆ **lattice defects**

O atoms in the ZrN latice

High reactive gas flow

⬇ **residual stress**

- **Formation poorly crystallized Oxygen doped Zr_3N_4 phase**
- **Formation oxynitride phases**

4. Results

4.8 Mechanical - Hardness

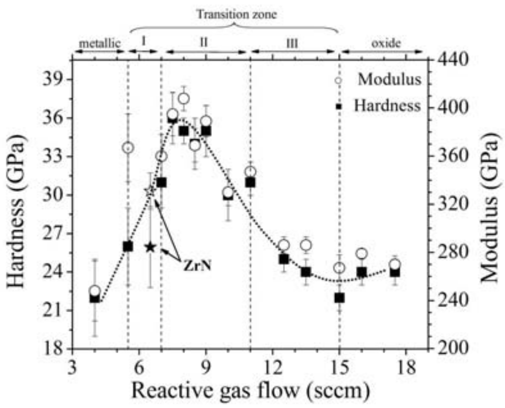

Low reactive gas flow

⬆ **hardness**

⬆ **lattice defects**

Zr atoms in the ZrN lattice

⬇ **dislocation motion**

High reactive gas flow

✓ **Formation of oxide phases.**

✓ **Formation poorly crystallized Oxygen doped Zr_3N_4 phase**

4. Results

4.9 Thermal annealing: Structure

- **As-deposited films revealed:**
  Films exhibit a **fcc ZrN**
  ≠ peak positions for ≠ samples:
  high compressive stress, could indicate **O in ZrN**

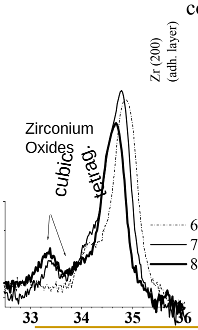

- Traces of crystallization appear at 700 and 800 ºC, possibly corresponding to cubic, tetragonal or cubic zirconium oxynitride.

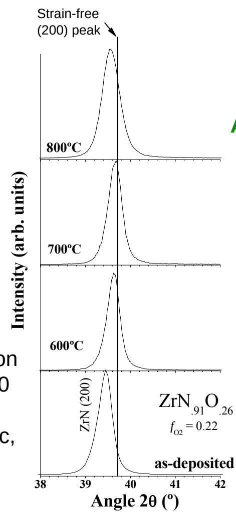

Annealed films revealed:

- the annealing up to 700 ºC induce stress relieves and structural relaxation of films
- during cooling, the differences in thermal expansion coefficients of films and substrates can induce "new" stress states.

4. Results

Thermal annealing:

Mechanical properties: *Hardness*

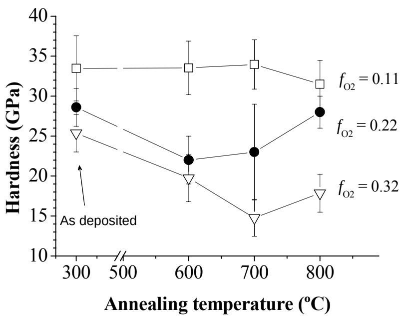

Results revealed:

- ❑ Nearly constant hardness at low oxygen fractions (0.10< f_{O2} <0.22) up to 800 ºC
- ❑ At intermediate and high f_{O2}, hardness decreases at lower temperatures:
  - ☑ structure recovery: dislocations annihilation, processing gases release, grain growth, etc.
- ❑ At intermediate and high oxygen content hardness increase at higher temperatures.
  - ☑ Formation of a nanostructured-type composite (nc-ZrN/a-oxides)
  - ☑ The O doping of ZrN (solid solution)

are hypothesis to be considered

5. Conclusions

- **Thin films within the Zr-O-N ternary system were prepared by dc reactive magnetron sputtering.**
- **Structural characterization revealed the existence of 3 different structures**
  - **fcc ZrN.**
  - **structure that might be similar to that of Zr_3N_4 with oxygen inclusions.**
  - **crystalline structures that were indexed as oxynitride phase.**
- **Colour characterization reveal the existence of 3 distinct zones, with direct relationship with the evolution of the 3 different's structures.**
- **Resistivity data reveal the existence of 2 distinct electrical behaviour, characteristic of the conductive fcc-ZrN and the semi-conductive/insolating electrical behavior of O-Zr_3N_4 and the oxynitrides phases.**
- **Infra red Absorption Spectroscopy data reveal a strong relationship between the structural evolution and chemical changes.**
- **Regarding colour of as-deposited films, it was observed a clear dependence of the obtained colorations with oxygen fraction.**
- **Hardness and residual stress measurements revealed higher values for the region with low oxygen contend.**

The authors gratefully acknowledge the financial support of the:

European Union through the NMP3-CT-2003-505948 project "HARDECOAT"

Portuguese FCT institution by the project nº POCTI/38086/CTM/2001 co-financed by European community fund FEDER.